JOURNAL OF RAMAN SPECTROSCOPY
J. Raman Spectrosc. **29**, 927–931 (1998)

Resonance Raman Examination of the Two Lowest Amide ππ* Excited States

Sanford A. Asher,* Zhenhuan Chi and Pusheng Li
Department of Chemistry, University of Pittsburgh, Pittsburgh, Pennsylvania 15260, USA

The UV Raman spectra of *N*-methylacetamide (NMA) were measured in H_2O and D_2O between the visible spectral region and the UV region down to 184 nm. The Raman excitation profiles indicate that all of the amide bands are resonance enhanced by the first dipole-allowed $\pi \rightarrow \pi^*$ transition at 190 nm. The Raman excitation profile data indicate the presence of destructive interference from the second allowed transition at *ca.* 165 nm. For example, the amide I and amide I′ bands disappear in the 184 nm UV Raman spectra and the relative intensities of the amide II and III bands change. The first allowed electronic transition at *ca.* 190 nm occurs to an excited ππ* state where the major geometry change, relative to the ground state, involves a dominating C—N bond elongation, with smaller C—C and N—C bond contractions, and a more modest C=O bond elongation. The C—N ground-state double bond character may decrease to the point where free rotation may occur. This may explain the previously observed monophotonic photoisomerization of *trans*-NMA to *cis*-NMA. The second allowed transition at *ca.* 165 nm occurs to an excited state whose major geometry change involves C=O bond elongation. © 1998 John Wiley & Sons, Ltd.

INTRODUCTION

The understanding of molecular electronic excited-state geometries is far murkier than is generally appreciated. Significant insight exists only for very small molecules such as H_2 and H_2O, where sufficiently few electrons occur that reliable calculations can apparently be performed to predict their excited-state structures. The situation is even more opaque for molecules dissolved in solvents, where the energies of the molecule's electronic transitions overlap those of the solvent.

Electronic absorption spectroscopy is the classical approach to obtaining qualitative information on excited-state geometries. Correlations of Franck–Condon envelopes with the ground electronic state normal modes of vibration can offer insight into the geometric distortions which occur upon electronic excitation. However, higher energy electronic absorption bands are often broad and display little vibrational fine structure.[1] This is especially true for condensed-phase samples. In addition, as excitation approaches the deep UV ($\lambda < 200$ nm), the absorption bands recede into the solvent absorption continuum.

For example, a critical perusal of the pre-1991 literature indicates that almost nothing was known about the geometry of the first ππ* transition of *N*-methyacetamide (NMA), a small but crucially important molecule.[2,3] This is the smallest molecular fragment which contains the monosubstituted amide group, which is the simplest appropriate model for the peptide bonds of proteins. This lacunae is especially troubling since it impedes deep insight into a variety of areas involving protein structure and function. For example, it will be difficult to develop detailed molecular insight into phenomena such as electron transfer in biology without a deep understanding of the electronic structure of the medium through which electron transfer takes place.

However, it should be noted that even in the absence of an understanding of the amide electronic excited-state geometry, significant progress was made in correlating protein secondary structure to oscillator strengths of these transitions; numerous workers have developed excitonic interaction models to explain the amide transition oscillator strengths of the different protein secondary structures. In addition, these approaches were crucial for the development of electronic circular dichroism as the standard protein secondary structure determination methodology.[4,5]

The ground state of NMA is well known to be planar owing to the partial double bond character of the C—N bond.[6] The lowest energy ground-state structure is *trans*, the *cis* planar conformation being *ca.* 3 kcal mol^{-1} (1 kcal = 4.184 kJ) higher in energy. Nearly 30 years ago, Scheraga's group[2] suggested that the lowest energy amide ππ* excited-state geometry should be twisted and elongated along the C—N bond, owing to interactions between the C=O π* orbital and the nitrogen non-bonding orbital. Li *et al.*,[7] motivated by our resonance Raman amide studies, performed *ab initio* calculations of the excited-state structure of NMA. They did not find a twisted amide excited-state geometry, but calculated that the amide N atom rehybridized to a tetrahedral geometry in the first allowed NMA ππ* state. This should result in free rotation about the C—N bond within the excited state.

* Correspondence to: S. A. Asher, Department of Chemistry, University of Pittsburgh, Pittsburgh, Pennsylvania 15260, USA
E-mail: asher + @pitt.edu
Contract/grant sponsor: NIH.
Contract/grant number: R01GM30741-14.

CCC 0377–0486/98/100927–05 $17.50

Received 16 April 1998
Accepted 13 June 1998

None of the work to date has determined the excited-state geometry bond lengths or force constants. Part of the problem is that the existing theoretical techniques are known not to be reliable for excited-state geometries of any but the smallest molecules. In addition, Li *et al.*'s calculation examined NMA in vacuum, and did not include the important hydrogen bonding linkages with water.

Recently, a number of groups have applied UV resonance Raman spectroscopy (UVRRS) to NMA in order to explore experimentally the excited-state geometries of the lowest energy electronic transitions.[8–17] The power of RRS is that it examines the coupling of the ground-state nuclear vibrations to the electronic excited-state potential function; a knowledge of the ground-state vibrational modes can be used to intuit information on electronic excited-state geometries. Resonance Raman spectra excited within strong electronic transitions generally show selective enhancement of those ground-state vibrations that distort the ground state towards the excited-state geometry.[8,10,11,16]

For NMA a number of surprises appeared from these initial UVRRS measurements. (1) The dominant bands enhanced involved C–N stretching and CH_3 umbrella bending. Little enhancement was evident for C=O stretching vibrations in water; however, in the gas phase or in non-hydrogen-bonding solutions, the C=O stretching vibration dominated.[8,16,17] At first glance these results suggested that dramatic differences occur between hydrogen-bonded and non-hydrogen-bonded NMA excited states. (2) The major aqueous NMA geometric change was C—N bond elongation. Enhancement of the C–H bending vibration was mysterious. (3) Non-hydrogen-bonded NMA appeared to have an excited state mainly elongated along the C=O bond. (4) The observed monophotonic isomerization of ground-state *trans*-NMA to ground-state *cis*-NMA within *ca.* 3 ns may be signaling a twisted amide $\pi\pi^*$ excited state.[8,10,11,16]

Our recent quantitative NMA studies demonstrated a dominating C—N bond elongation and a contraction of the C—C and N—C bonds, with a variable elongation of the C=O bond, depending upon whether NMA was in aqueous solution, in non-bonding hydrogen-bonding solvents or in the gas phase.[8] We rationalized most of the difference in C=O enhancement in hydrogen-bonded *vs.* non-hydrogen-bonded NMA as resulting from ground-state C=O bond elongation upon hydrogen bonding to water, in combination with the resulting ground-state normal mode changes. We detected only a modest difference in the 190 nm $\pi\pi^*$ excited state between hydrogen-bonded and non-hydrogen-bonded NMA. These studies probed down to 190 nm, well into resonance with the first amide $\pi\pi^*$ state. We found no evidence of enhancement of torsional modes which might accompany excited-state twisting.

Hudson's group calculated an NMA excited-state geometry which yielded calculated[18] UVRR spectra similar to those measured experimentally.[17] The aqueous geometries were similar to those we determined experimentally. However, they concluded that large excited-state geometry differences occur between the hydrogen-bonded and non-hydrogen-bonded first $\pi\pi^*$ state. For example, they calculated that the ratio of C=O to C—N bond elongation was *ca.* fivefold larger for non-hydrogen-bonded NMA compared with NMA in water.

Wang and co-workers[15,16] measured the aqueous NMA Raman excitation profile deeper into the UV region down to 184 nm, past the maximum of the first amide $\pi \rightarrow \pi^*$ transition, and concluded that the amide excited-state characteristics and their energies were highly dependent upon hydrogen bonding, and that the first two amide $\pi\pi^*$ states reversed their order in non-hydrogen-bonded solutions. They suggested that this accounted for the large UVRRS differences observed between different solvents.

If the amide excited-state energies and geometries, indeed, depend dramatically on amide hydrogen bonding, this will severely complicate any picture of protein excited states; a protein would not then be made up of similar linked amide group fragments with similar electronic excited-state properties, but instead the electronic excited states of these fragments would differ dramatically depending upon their hydrogen bonding.

Because of the central importance of the understanding of NMA excited states for all future studies of amides, peptides and proteins, we have reinvestigated the UV Raman spectra and excitation profiles of NMA. We show here that these new results confirm our earlier excited-state geometry assignments of NMA. We also find that the second $\pi\pi^*$ state of NMA is probably dominated by a C=O bond elongation.

EXPERIMENTAL

The 206 nm spectra were excited by a cw frequency-doubled Kr^+ laser. The 200 and 184 nm excitation wavelength derived from a quadrupled Coherent Infinity 100 Hz YAG laser which was Raman shifted three and four anti-Stokes harmonics in H_2, respectively. Further details on the experimental set-up are described elsewhere.[13] The 184 nm measurements (average power 0.4 mW) were extremely challenging; these measurements required nitrogen purging and the use of a single spectrograph. The data were analyzed as described previously. Detailed information on the 184 nm measurements can be found in Asher *et al.*[13]

RESULTS AND DISCUSSION

Figure 1 shows the UVRR spectra of NMA in H_2O and in D_2O (NMAD) at 206, 200 and 184 nm. For NMA in water we see strong enhancement of the amide II and III bands, which involve large contributions of C–N stretching and N–H bending, in addition to enhancement of the 1380 cm^{-1} C–H sb, which involves CH_3–C umbrella motion. We demonstrated earlier that this C–H sb band enhancement is derived from its significant C–C stretching composition.[8] The amide I C=O stretching band is weak and only appears as a *ca.* 1620 cm^{-1} shoulder. The NMAD spectrum differs dramatically because the N–D bending decouples from C–N stretching, which leaves a single dominating *ca.* 1500

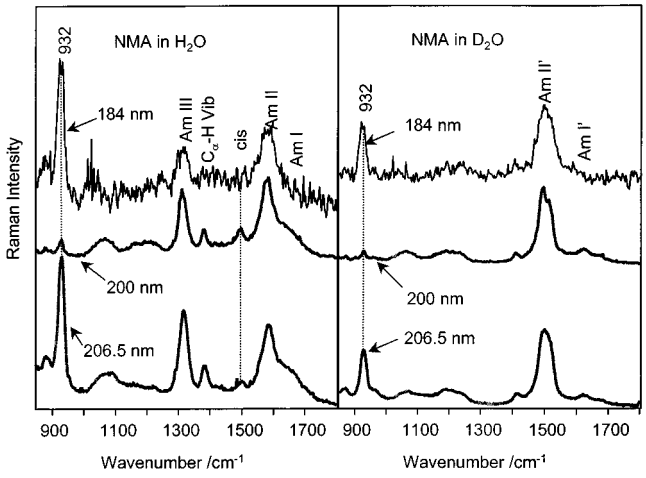

Figure 1. UV resonance Raman spectra of *N*-methylacetamide (NMA) and *N*-deuteriated *N*-methylacetamide (NMAD) at 206.5 nm (10 mM), 200 nm (10 mM) and 184 nm (4 mM) in aqueous solution containing 0.5 M sodium perchlorate. The spectral resolution for 206.5 and 200 nm excitation is 8 cm^{-1} and for 184 nm it is 24 cm^{-1}. Comparison between the 184 nm excited spectra and those at longer wavelength indicates that the amide I and amide I′ bands disappear with 184 nm excitation.

cm^{-1} amide II′ C–N stretching band. The weak amide I′ band can now be easily observed in all but the 184 nm UVRR spectrum, where it disappears.

As the excitation shifts from *ca.* 244 to 190 nm, the relative amide band intensities remain almost constant (Fig. 2). However, the amide I′ band (and also the amide I band shoulder) disappears with 184 nm excitation. These decreased Raman cross-sections are clearly seen in the Fig. 2 excitation profiles of NMA and NMAD, which also display the amide I/amide II and amide I′/amide II′ relative Raman cross-section ratios.

The fact that all of the amide band excitation profiles, including those of the amide I and I′ bands, show maxima at *ca.* 190 nm indicates that these bands are enhanced by the lowest energy amide 190 nm $\pi \rightarrow \pi^*$ transition. Further, the unique amide I and amide I′ band disappearance at the shortest wavelength and the decreased intensities for the other amide bands indicate the presence of resonance Raman destructive interference,[19,20] due to the contribution to the Raman tensor of the next strongly allowed $\pi \rightarrow \pi^*$ electronic transition (at 165 nm?). This observation of destructive interference is consistent with our earlier preresonance Raman depolarization ratio dispersion measurements;[21] as excitation approached the first amide $\pi \rightarrow \pi^*$ transition, the amide I′ depolarization ratio uniquely decreased below 0.33, which is consistent with at least two transitions contributing to preresonance enhancement.

The facts that the preresonance Raman depolarization ratio is smaller than 0.33 and that we observe destructive interference with excitation between the two transitions indicate that these transitions contribute to the Raman polarizability with the same sign. This also indicates that the products of their transition moments and Franck–Condon factors in the KHD expression are of the same sign in preresonance. As excitation passes through the amide $\pi \rightarrow \pi^*$ transition, the resonance Raman tensor components change sign.[20] The complete amide I band destructive interference suggests that the second $\pi\pi^*$ excited state is preferentially elongated along the C=O bond.

The sharp excitation profile decrease at shorter wavelength excitation suggests that the other amide bands may also suffer destructive interference. The excitation profiles indicate that the NMA amide III band intensity decreases faster than that of the amide II band at shorter excitation wavelengths. This contrasts sharply with their behavior at longer wavelengths where the amide III/II band relative intensities are almost constant.

The magnitude of destructive interference will differ for the amide II and III bands, since their vibrational compositions differ.[8] The amide II and III bands are both enhanced by the 190 nm $\pi\pi^*$ excited state, because they contain significant C–N, C=O, C–C and N–C motion; the excited state is dominantly expanded along the C—N bond, significantly contracted along the C—C and N—C bonds and expanded somewhat along the C=O bond. However, the amide II and III band eigenvectors quantitatively differ in C–N and C=O stretching composition. In addition, the phasing of the vibrations differ; the amide III vibration involves simultaneous C–N and C=O stretching, while the amide II vibration has C–N stretching accompanied by C=O contraction.[8]

The more pronounced amide III destructive interference can be qualitatively rationalized from this phasing difference in their motions. As excitation occurs between the 190 and 165 nm transitions, both transitions contribute to resonance enhancement. The absolute signs of the Raman tensor elements cannot be determined, but the relative signs can be predicted.[22] For argument we will assume positive signs for the preresonance Raman tensor elements contributed by the 190 and 165 nm transitions. The tensor elements contributed by the 190 nm $\pi \rightarrow \pi^*$ transition become negative for excitation wavelengths below 190 nm, while the sign of the contribution of the 165 nm transition remains positive. Thus, for the amide III band, significant cancellation could occur between the 165 nm enhancement and the 190 nm enhancement of the C–N and C=O coordinate stretching components. In contrast, the amide II phasing difference for C=O stretching and C–N stretching would lead to less destructive interference. All of these results are consistent with a picture that the 165 nm second $\pi \rightarrow \pi^*$ transition is mainly elongated along the C=O bond. This picture utilizes the standard assumption that resonance enhancement results from the Raman Franck–Condon factors. In this approximation, we neglect the influence of bond force constant changes.

Our measured excitation profiles differ dramatically from that of Wang and co-workers,[15,16] as discussed in detail elsewhere.[13] For excitation at $\lambda > 190$ nm Wang *et al.*'s measurements are flawed because they did not correct for self-absorption. For $\lambda < 190$ nm we believe their data are spurious.

Our results presented above clearly indicate that the UVRR spectra of NMA and NMAD excited between 190 and *ca.* 240 nm are dominated by the *ca.* 190 nm $\pi \rightarrow \pi^*$ transition. This fulfils the condition for our previous use of simple resonance Raman theory to calcu-

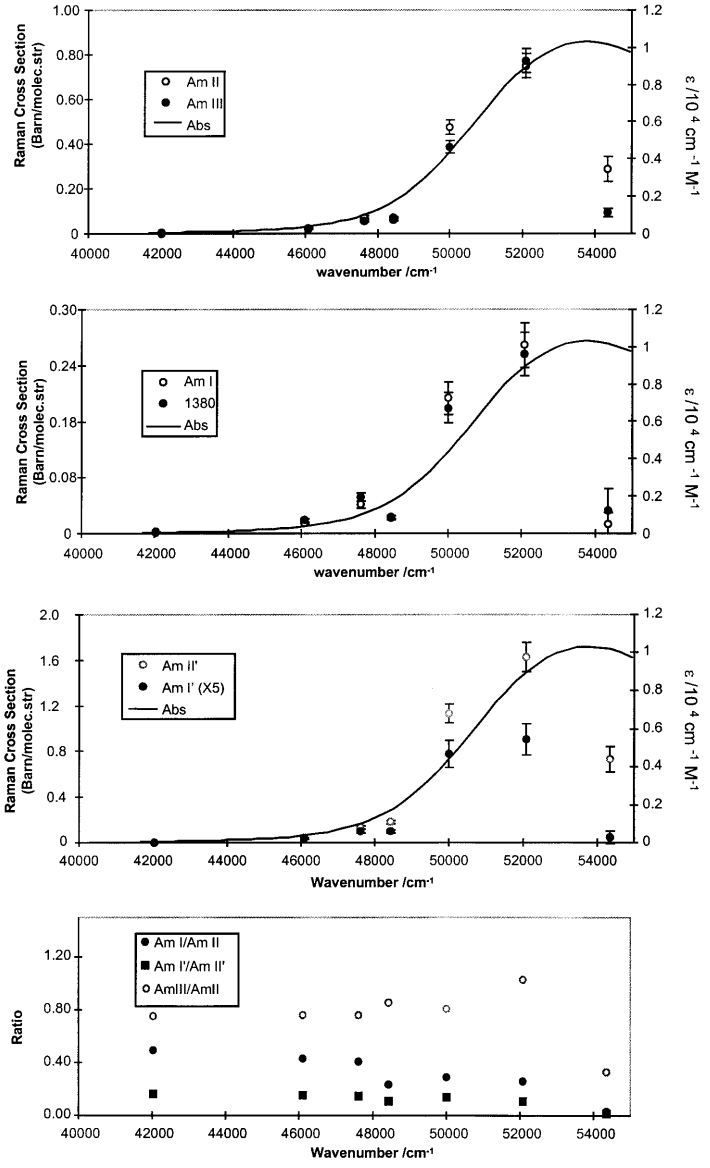

Figure 2. UV Raman excitation profiles of NMA and NMAD showing an excitation profile peak at *ca.* 190 nm. Below 190 nm the amide II′ cross-section decreases more than twofold, while the amide I′ band disappears. The bottom panel shows the excitation wavelength dependence of the amide I/amide II and the amide I′/amide II′ band Raman cross-section ratios. The cross-sections for the amide I and II bands were determined by peak deconvolution after subtracting the contribution of water. All excitation profile data were corrected for self-absorption by measuring spectra in the presence of 5% CH_3CN. The self-absorption correction factors were determined from the ratio of the acetonitrile band cross-sections. We compared the spectra of acetonitrile in the presence and absence of NMA with those in 5% CH_3CN, H_2O (D_2O) and ClO_4^- solutions. The observed spectra were corrected for the spectrometer throughput efficiency. The $\lambda > 206$ nm data derive from Chen *et al.*[8]

late excited-state geometries. This assumption is supported by Markham and Hudson's recent excited-state NMA geometry calculations,[18] which gave similar results by calculating UVRRS from excited-state equilibrium geometry displacements or from gradients. The remaining assumption used is that the major excited-state potential function changes are associated with displacements.

We conclude that the first allowed $\pi\pi^*$ excited state of NMA in water is mainly displaced along the C—N bond, with a C=O displacement which is *ca.* threefold less. Our results indicate that for gas-phase NMA the C=O displacement becomes comparable to that of the C—N, but our results are inconsistent with the threefold larger elongation calculated by Markham and Hudson.[18]

CONCLUSIONS

The first allowed electronic transition at *ca.* 190 nm of amides such as NMA in water occurs to an excited state where the major geometry change relative to the ground state involves a dominating C—N bond elongation, with smaller C—C and N—C bond contractions and a more modest C=O bond expansion. The C—N double

bond character decreases to the point where free rotation occurs and may permit photoisomerization to *cis*-NMA. The second allowed transition at *ca.* 165 nm occurs to an excited state whose major geometry change involves C=O bond elongation.

Acknowledgements

We gratefully acknowledge support from NIH grant R01GM30741-14 to S.A.A. We also thank Professor Samuel Krimm for helpful discussions.

REFERENCES

1. M. B. Robin, *Higher Excited States of Polyatomic Molecules*. Academic Press, New York (1974).
2. J. F. Yan, F. A. Momany, R. Hoffmann and H. A. Scheraga, *J. Phys. Chem.* **74**, 420 (1970).
3. J. A. Ryan and J. L. Whitten, *J. Am. Chem. Soc.* **94**, 2396 (1972).
4. W. C. Johnson, Jr, *Proteins: Struct. Funct. Genet.* **7**, 205 (1990).
5. (a) R. W. Woody, *Methods Enzymol.* **246**, 34 (1995); (b) N. J. Greenfield, *Anal. Biochem.* **235**, 1 (1996).
6. J. L. Katz and B. Post, *Acta Crystallogr.* **13**, 624 (1960).
7. Y. Li, R. L. Garrell and K. N. Houk, *J. Am. Chem. Soc.* **113**, 5895 (1991).
8. X. G. Chen, S. A. Asher, R. Scheitzer-Stenner, N. G. Mirkin and S. Krimm, *J. Am. Chem. Soc.* **117**, 2884 (1995).
9. X. G. Chen, R. Scheitzer-Stenner, S. A. Asher, N. G. Mirkin and S. Krimm, *J. Phys. Chem.* **99**, 3074 (1995).
10. S. Song, S. A. Asher, S. Krimm and K. D. Shaw, *J. Am. Chem. Soc.* **113**, 1155 (1991).
11. P. Li, X. G. Chen, E. Shulin and S. A. Asher, *J. Am. Chem. Soc.* **119**, 1116 (1997).
12. J. M. Dudik, C. R. Johnson and S. A. Asher, *J. Phys. Chem.* **89**, 3805 (1985).
13. S. A. Asher, P. Li, Z. Chi, X. G. Chen, R. Schweitzer-Steinner, N. G. Mirkin and S. Krimm, *J. Phys. Chem.* **101**, 3992 (1997).
14. S. Song and S. A. Asher, *J. Am. Chem. Soc.* **111**, 4295 (1989).
15. Y. Wang, R. Purrello, S. Georgiou and T. G. Spiro, *J. Am. Chem. Soc.* **113**, 6359 (1991).
16. Y. Wang, R. Purrello, T. Jordan and T. G. Spiro, *J. Am. Chem. Soc.* **113**, 6368 (1991).
17. L. C. Mayne and B. S. Hudson, *J. Phys. Chem.* **95**, 2962 (1991).
18. L. M. Markham and B. S. Hudson, *J. Phys. Chem.* **100**, 2731 (1996).
19. P. Stein, V. Miskowski, W. H. Woodruff, J. P. Griffin, K. G. Werner, B. P. Gaber and T. G. Spiro, *J. Phys. Chem.* **64**, 2159 (1976).
20. J. Friedman and R. Hochstrasser, *Chem. Phys. Lett.* **32**, 414 (1975).
21. X. G. Chen, P. Li, J. S. W. Holtz, Z. Chi, V. Pajcini, S. A. Asher and L. A. Kelly, *J. Am. Chem. Soc.* **118**, 9705 (1996).
22. V. Pajcini, X. G. Chen, R. W. Bormett, S. J. Geib, P. Li, S. A. Asher and E. G. Liediak, *J. Am. Chem. Soc.* **118**, 9716 (1996).